

One-step synthesis of dye-incorporated porous silica particles

Qing Liu · Philip DeShong · Michael R. Zachariah

Received: 30 January 2012 / Accepted: 10 May 2012 / Published online: 24 June 2012
© Springer Science+Business Media B.V. 2012

Abstract Fluorescent nanoparticles have a variety of biomedical applications as diagnostics and traceable drug delivery agents. Highly fluorescent porous silica nanoparticles were synthesized in a water/oil phase by a microemulsion method. What is unique about the resulting porous silica nanoparticles is the combination of a single-step, efficient synthesis and the high stability of its fluorescence emission in the resulting materials. The key of the success of this approach is the choice of a lipid dye that functions as a surrogate surfactant in the preparation. The surfactant dye was incorporated at the interface of the inorganic silica matrix and organic environment (pore template), and thus insures the stability of the dye–silica hybrid structure. The resulting fluorescent silica materials have a number of properties that make them attractive for biomedical applications: the availability of various color of the resulting nanoparticle from among a broad spectrum of commercially dyes, the controllability of

pore size (diameters of ~ 5 nm) and particle size (diameters of ~ 40 nm) by adjusting template monomer concentration and the water/oil ratio, and the stability and durability of particle fluorescence because of the deep insertion of surfactant's tail into the silica matrix.

Keywords Silica · Fluorescence · Dyes · Porous particles

Introduction

Silica material is used in a variety of biological applications because of its resistance to microbial attack, stability in aqueous solutions, low toxicity, ability to be functionalized, and penetrability through biomembranes (Bharali et al. 2005; Wang et al. 2009). Porous silica is particularly attractive due to the potential to transport drugs within the dead volume of the porous particles (Wang et al. 2009). Common synthesis methods for the production of porous silica include templating (Capek 2010) and co-condensation (Huh et al. 2003) with organoalkoxysilanes.

For many applications, such as diagnostics and drug delivery, bright and stable luminescent labels are often required. Labeling methods include quantum dots, metal nanoparticles, and doping dyes or chromophores (Yao et al. 2006). Because of biodegradation and toxicity issues associated with quantum dots, (Michalet et al. 2005) dye labeling of nanoparticles has been

Electronic supplementary material The online version of this article (doi:10.1007/s11051-012-0923-4) contains supplementary material, which is available to authorized users.

Q. Liu · P. DeShong · M. R. Zachariah (✉)
Department of Chemistry and Biochemistry, University
of Maryland, College Park, MD 20742, USA
e-mail: mrz@umd.edu

M. R. Zachariah
Department of Mechanical Engineering, University
of Maryland, College Park, MD 20742, USA

drawing recent attention. Research on the use of dye-functionalized nanoparticles has focuses on photostability of the dye, leakage of the dye from the matrix, and chemical stability of the matrix.

Several types of approaches to synthesize the luminescent-labeled silica nanoparticles have been reported. A typical approach to mitigate some of these problems is to encapsulate the dye within silica during particle formation and to employ electrostatic forces to assemble the cationic dye within the silica matrix (Shibata et al. 1997). However, due to the weakness of the electrostatic forces acting on the dye molecules in typical nanoparticle systems, an alternative method for preparing bright, stable nanoparticles is to modify the organic dye to make it more hydrophilic, and thus increase its affinity of the dye for the matrix (Zhao et al. 2004). To promote a stronger attachment, the dye is modified so it can be directly linked with organosilanes participating in the co-condensation process with the primary silica precursor, typically tetraethoxysilane (TEOS) (Vanblaaderen and Vrij 1992). What is trying to be improved can be the weak electrostatic assemble or the complicated modification of the dye precursor. However, the complicated modification of the dye precursor and the weak electrostatic assemble obstruct the wide application of the methods.

A second strategy for the preparation of fluorescent silica nanoparticles is to add the dye after the silica matrix has been created and allow the dye to become incorporated into the organic matrix by diffusion. Post-treatment can be accomplished either by wet impregnation, whereby the dye is physically absorbed onto the pre-synthesized porous silica material, or as a post-graft method, to chemically bond the dye to the matrix in a second step (Li et al. 2010). Beyond the added functionality that a fluorescent silica particle may offer, the silica matrix itself serves to isolate the dye from outside environment such as solvent, oxygen, and free radicals caused by light exposure (Xie et al. 2010) and protect dye molecules from photodecomposition. In addition, using low concentration of bound dye has in some cases been shown to increase the relative quantum yield relative to a free dye due to lower self-quenching (Ma et al. 2009). However, these methods suffer from dye leakage unless chemical bonding is employed (Gao et al. 2009) or by addition of an additional silica capping layer to trap the dye in a core-shell structure (Rocha et al. 2010). The methods

described above can be categorized as either a one-step methods which may suffer from poor fixing of the dye or multi-step methods that enjoy greater dye stability at the cost of synthetic complexity.

Another class of materials is to combine fluorescence with a porous structure. As in the solid particle cases, synthesis of fluorescent porous particles is typically a multi-step process (Wang et al. 2010; Stein et al. 2000; Tsyalkovsky et al. 2008; Guli et al. 2007). Also, these methods cannot independently control pore structure due to the employment of surfactant as pore template in the process of synthesis.

In this work, we introduce a one-step method to label porous silica nanoparticles (PSN) with fluorescent dyes using polystyrene (PS) as the extensive pore template, cetyltrimethylammoniumbromide (CTAB) as a micelle template (Nandiyanto et al. 2009), and an embedding "lipid" dye. This approach also allows us to independently control both pore and particle size. The use of a lipid dye enables the dye to function as a surrogate surfactant with the primary surfactant (CTAB) on the organic and inorganic interface. From BET analysis, by washing off the PS and micelle templates, particle surface area is increased for potential drug loading or subsequent modification without eliminating the fluorescent effectiveness. Two different dyes were studied, both independently and in combination to demonstrate the reliability of the method.

Experimental

Materials

The materials used are: TEOS (98 %, Aldrich) as the silica precursor; L-lysine (Aldrich) as the catalyst for silica size control; (Thomassen et al. 2010) styrene monomer (Aldrich) as the template monomer, stabilizer removed before use; CTAB (Aldrich) as necessary template and surfactant; 2,2'-Azobis (2-methylpropionamide) dihydrochloride (AIBA, Aldrich) as the initiator of styrene polymerization; octane (Aldrich, 98 %) and distilled water to make oil/water reaction system; and 1,2-dioleoyl-*sn*-glycero-3-phosphoethanolamine-*N*-(lissamine rhodamine B sulfonyl) ammonium salt (Liss Rhod PE, dye LR, Avanti Polar Lipids, in chloroform), 1,2-dioleoyl-*sn*-glycero-3-phosphoethanolamine-*N*-(5-dimethylamino-1-naphthalenesulfonyl) ammonium salt (Dansyl PE, dye D, Avanti Polar Lipids,

in chloroform), Coumarin 440 (dye C, Exciton Chemical Company, Inc., Dayton, OH), and Rhodamine 590 (dye R, Exciton Chemical Company, Inc., Dayton, OH) as fluorescent sources.

Synthesis of fluorescent mesoporous silica nanoparticle

A typical synthesis of the fluorescent mesoporous silica nanoparticles is described as follows. First, about 0.3 mL dye solution (1 mg/mL in chloroform) were added to a solution of 0.050 g CTAB in 15 mL of H₂O heated to 60 °C in a three-necked flask reactor. Then, 0.15 g of styrene, 0.011 g of lysine, 0.50 g of TEOS, 5.1 g of octane, and 0.013 g of AIBA were subsequently added to the system. The homogeneous reaction mixture was stirred under N₂ at 60 °C for 3 h. After cooling, the resulting suspension was decanted from the fluorescent nanoparticles that had formed. The sample was subjected to sonication in ethanol followed by centrifugation for three times to insure that excess surfactant and unincorporated dye were removed. Finally, the polystyrene template was removed by sonication-centrifugation with tetrahydrofuran (THF) for three times (Lee et al. 2011). Particles were collected by centrifugation and dried in the air.

Silica nanoparticles without polystyrene template (no-PS PSN) were prepared according to the same recipe except that styrene and AIBA addition was omitted. Synthesized according to the above procedure, PSN-LR, PSN-D, PSN-C, and PSN-R are porous silica nanoparticle incorporated with Liss Rhod PE, Dansyl PE, Coumarin 440, and Rhodamine 590, respectively; PSN-LR and D is incorporated with Liss Rhod PE and Dansyl PE in combination.

Characterization

UV–Vis absorption and fluorescent spectra of the solid product were obtained using a Lambda 850 UV–Vis and Cary Eclipse fluorescent spectrophotometer, respectively. Transmission electron microscopy (TEM) was performed on a JEOL JEM 2100 FEG instrument. Pore size and porosity measurements were performed by the Brunauer-Emmett-Teller (BET) method on a Micrometrics TriStar II 3020 instrument.

Results and discussion

We chose a lipid-like dye for these experiments so as to enable the dye to also serve as a surrogate surfactant in conjunction with the primary surfactant CTAB to increase the fixing efficiency of the particle formation. Under either ambient or UV light, it was quite clear that the dye was successfully embedded in the particles. Furthermore, subsequent washing and centrifugation, showed little color in the supernatant indicating that this approach is quite efficient at incorporation of the dye into the matrix. To test for long term stability of the fluorescent emission from the particles, the particles were kept in a water solution for a period of up to 6 months. No fluorescent degradation was detected, indicating that the particles were photostable with minimal dye leakage.

Two additional dyes were chosen for control experiments. Coumarin 440 is non-ionic dye and Rhodamine 590 is an ionic dye; neither of which have a Liss Rhod PE's surrogate-surfactant structure. (Dye structures are shown in Fig. 1.) Since PSN-C and PSN-R were not the subjects of this study, luminescent characterization was not conducted for the resulting nanoparticles.

Figure 2a and b show the fluorescence associated with the supernatant and the silica nanoparticles from the first washing, respectively. It is clear from these photos that all the four dyes can be incorporated into the particle, resulting in all dye-PSNs with significant luminescence. However, dye incorporation efficiencies are different: when PSN-LR and PSN-D were washed, the supernatants are almost colorless; when PSN-C and PSN-R were washed, dyes dissolve into the ethanol solution. Also, as PSN-C and PSN-R were washed many times, the supernatants show a more diminished color, as well as the particles, indicating that the organic Coumarin 440 and ionic Rhodamine 590 end up in the ethanol extracts rather than in the silica matrix.

Figure 3 is a TEM image of the porous silica particles prepared by this method. While the particles are essentially monodispersed, we observe that the diameter of the nanoparticles prepared with the presence of PS (~40 nm) is larger than that of particles prepared without PS (~30 nm). Also, the former particles have a more ordered pore structure, extending deeper to the center of the particle (Dye addition or not would make no structure difference).

Fig. 1 Molecular structure of **a, b** lipid dyes, **c** small molecule nonionic dye and **d** small molecule ionic dye. (molecular structures are from <http://www.avantilipids.com/> and <http://www.exciton.com/>)

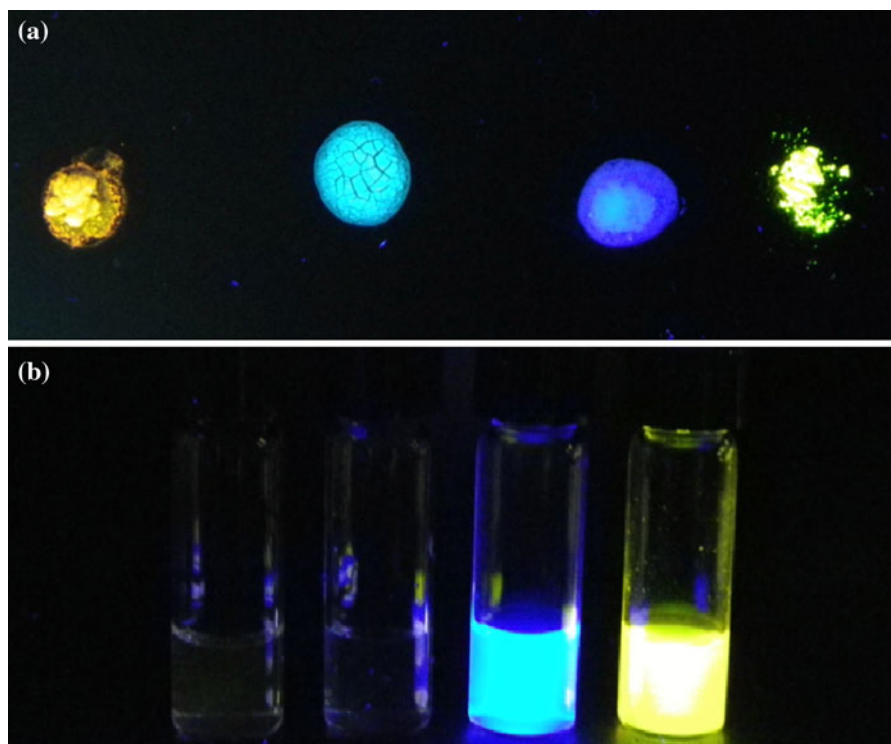
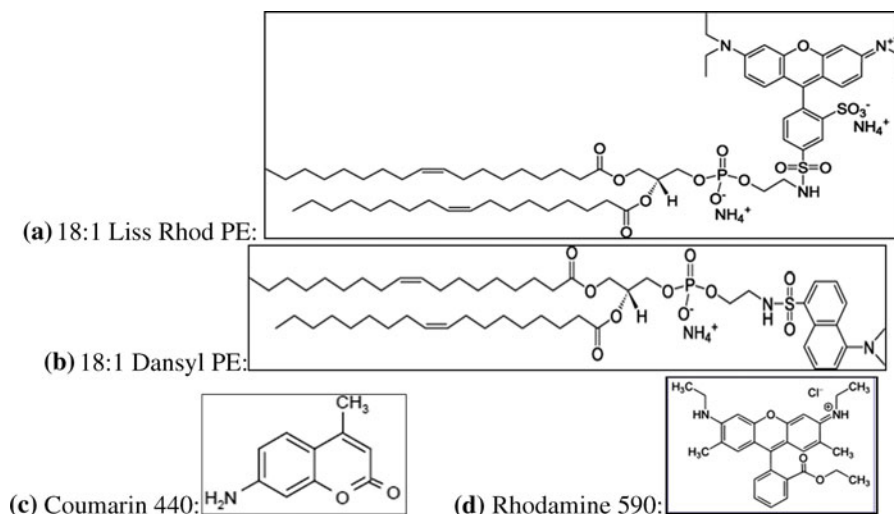


Fig. 2 From left to right: (under UV light) **a** PSN-LR, D, C and R spots on a slide and **b** supernatants of washing solvent of the same order after centrifugation

The porous structure was formed because of the addition of PS and CTAB, which also controlled the size distribution of the pores and the particles (Nandiyanto et al. 2009). It has been reported that surfactant and polymer form hybrid thread-like micelles in aqueous solution (Nakamura et al. 2003). In case

when dye is added, styrene addition forms the dye-colored hybrid polymer–surfactant (P–S) template, and thus creates a more uniform and dense porous structure, which is also responsible for a larger porosity and larger diameter of particles. In the absence of PS, the morphology of the particles is

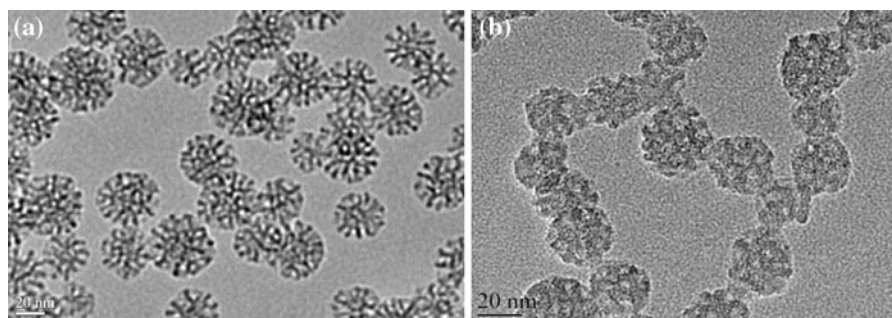


Fig. 3 TEM image of **a** PSN-LR and **b** no-PS PSN

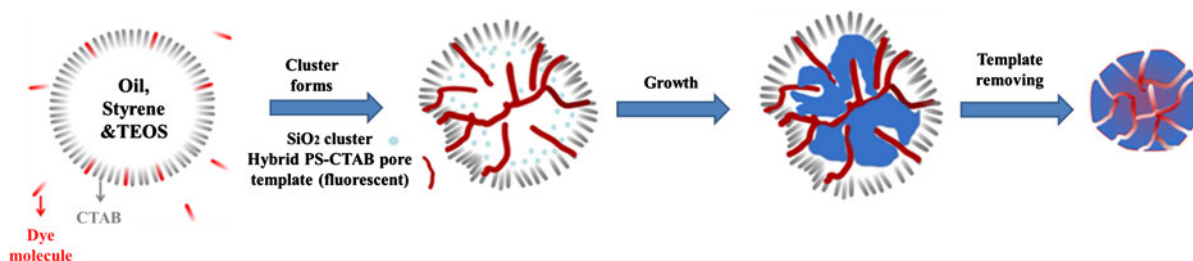


Fig. 4 Proposed mechanism of dye incorporation and porous silica formation

Table 1 Experimental fluorescence-emission wavelengths of solid dye(s) and dye-PSNs

Particle name	Embedded dye	Fluorescent emission wavelength of dye	Fluorescent emission wavelength of dye-PSN
PSN-LR	Liss Rhod PE (LR)	587 nm (ex: 557 nm) (Quemeneur et al. 2008)	564 nm (ex: 350 nm)
PSN-D	Dansyl PE (D)	510 nm (ex: 340 nm) (Christensen et al. 2001)	476 nm (ex: 340 nm)
PSN-LR and D	Liss Rhod PE and Dansyl PE (LR and D)	N/A	485, 530 and 573 nm (ex: 400 nm) 585 nm (ex: 350 nm)

different, obtained by comparing TEM images of Fig. 3a, b., since the silica cluster is negatively charged, and CTAB is a cationic surfactant, it is not unexpected that the P-S hybrid micelle or CTAB itself can be attracted to the silica matrix to make potential pore structure.

The proposed mechanism of dye-incorporated porous silica particle formation is shown in Fig. 4. The choice of a lipid dye is predicated on choosing something that has a surfactant-like head-tail structure so it can intercalate with CTAB to make dye-containing micelles. It is observed experimentally that the lipid dye LR is insoluble in octane, but it

dissolves when CTAB is added, which demonstrates that it can intercalate with CTAB. Initially, styrene and TEOS are oil soluble (inside micelle); lipid dye molecules transport into the micelle with the help of CTAB to form P-S pore template. Electrostatically, the cationic surfactant CTA^+ can also prevent the anionic dye X^- from dimerizing, (He et al. 2009) and thus self-quenching. The particle then grows due to electrostatic attraction of hybrid pore template and silica cluster until TEOS is completely consumed. For post-treatment, traditional calcination to eliminate the template cannot be applied here because it would destroy the fluorescence of the dye. Instead, ethanol

and THF are chosen to wash out the CTAB and pore template PS for two features: first, the long hydrophobic tail of the dye molecule can be trapped tightly in the structure, which prevents it from being washed out; second, removing the pore template by washing is more efficient for the pore structure closer to the surface because it takes time for deeply trapped molecules to diffuse out of the matrix and escape the particle.

The porous structure was also studied by BET-specific surface area characterization. With the same particle generation procedure, except for the dye addition, particle structures are the same under TEM, however, a calcination post-treatment could yield a surface area of about $600 \text{ m}^2/\text{g}$ (Nandiyanto et al. 2009), compared to a BET surface area of about $200 \text{ m}^2/\text{g}$ for the as-produced particles after removing the pore template by washing. Despite the fact that not all the template could be removed, this surface area is much larger than the theoretical surface area of a solid 40 nm silica particle ($12.8 \text{ m}^2/\text{g}$) (Table 1).

Fluorescence spectra of dye-PSNs are shown in Fig. 5. Because of inherent limit of fluorescence spectroscopy, (Evanko 2009) the ensuing results are only qualitative. PSN without dye has no fluorescence-emission peak, which can be taken as the background for the fluorescence label. (in Supplementary Fig. 2) Because the only difference between these samples is whether there is incorporated dye(s), the fluorescence peaks must originate from the dyes. Figure 5a–d show emission spectra of PSN-LR, PSN-D and PSN-LR, and D excited by the optimized excitation wavelength to obtain strong emission. In spite of the existence of both blue shift, comparing to the emission wavelength of fluorescent dyes, 587 nm at excitation of 557 nm (Quemeneur et al. 2008) for dye LR and 510 nm at excitation of 340 nm (Christensen et al. 2001) for dye D, high fluorescence at 564 and 476 nm for PSN-LR and PSN-D confirms the efficient single dye incorporation into the PSN.

The fluorescence spectrum of PSN-LR and D is more complicated, and is presented in Fig. 5c and d. Excitation at 350 nm results in one emission peak at 585 nm similar to what is seen for PSN-LR, but no peak is consistent with the emission of PSN-D. However, excitation at 400 nm gives three emission bands at 485, 530, and 573 nm. There are two possible reasons for this behavior. One is that LR absorbs strongly at 350 nm relative to D or alternatively

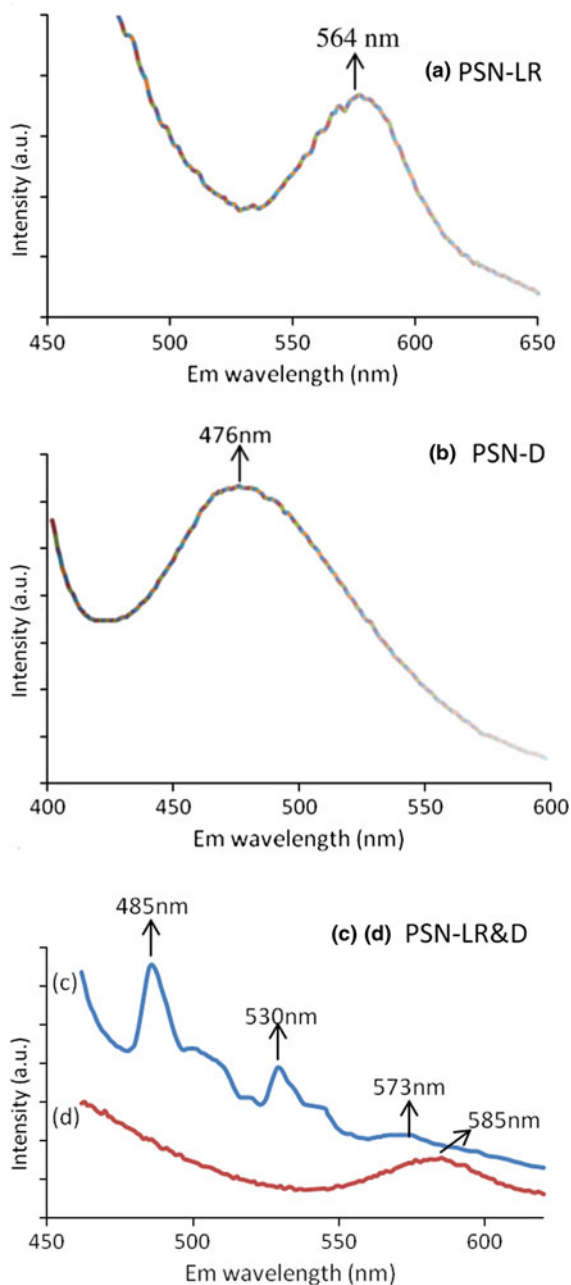


Fig. 5 Fluorescence spectra of **a** PSN-LR at excitation of 350 nm, **b** PSN-D at excitation of 340 nm, **c** and **d** PSN-LR and D at excitation of 400 nm and 350 nm

emission from dye D is reabsorbed by LR. In either case there appears to be significant quenching in emission as the quantum yield is much lower when the two dyes are mixed. This latter result may be a generic problem in trying to mix more than one dye within a particle.

Conclusions

A single-step, efficient method to synthesize photo and chemically stable dye-doped porous silica nanoparticles has been developed. The resulting nanoparticles are highly fluorescent and this method is applicable to the production of virtually any “color” of nanoparticle for which the corresponding dye is available. Encapsulating dyes into nanoparticles can stabilize dyes within the matrix, thus preventing aggregation and fluorescent quenching. The particle and pore sizes are controllable by adjusting the o/w ratio, surfactant concentration, and the amount of styrene; pore template PS could be removed for potential drug loading applications. What is unique for this method is that, compared to the non-chemical bonded dye doping methods nominally used for cationic dyes, (Shibata et al. 1997; Grasset et al. 2008) our fluorescent yield remained constant and dye leakage was negligible. Compared to the strong bonded dye doping method, this method is synthetically easier and without the need for toxic precursors (Nan et al. 2008).

Acknowledgments The generous financial support of the National Science Foundation (CHE 0511219478) is acknowledged. Partial support for characterization of the nanomaterials was provided by the University of Maryland-MERSEC Center. Q.L. also thanks Xiao Zhang from Rutgers University for the optical characterization.

References

- Al-Shamiri HAS, Kana MTH (2010) Laser performance and photostability of rhodamin B in solid host matrices. *Appl Phys B Laser Optic* 101(1–2):129–135. doi:10.1007/s00340-010-4192-6
- Bharali DJ, Klejbor I, Stachowiak EK, Dutta P, Roy I, Kaur N, Bergey EJ, Prasad PN, Stachowiak MK (2005) Organically modified silica nanoparticles: a nonviral vector for in vivo gene delivery and expression in the brain. *Proc Natl Acad Sci USA* 102(32):11539–11544. doi:10.1073/pnas.0504926102
- Capek I (2010) On inverse miniemulsion polymerization of conventional water-soluble monomers. *Adv Colloid Interface Sci* 156(1–2):35–61. doi:10.1016/j.cis.2010.02.006
- Christensen K, Bose HS, Harris FM, Miller WL, Bell JD (2001) Binding of steroidogenic acute regulatory protein to synthetic membranes suggests an active molten globule. *J Biol Chem* 276(20):17044–17051. doi:10.1074/jbc.M100903200
- Evanko D (2009) Primer: fluorescence imaging under the diffraction limit. *Nat Methods* 6(1):19–20. doi:10.1038/NMETH.F.235
- Gao XQ, He J, Deng L, Cao HN (2009) Synthesis and characterization of functionalized rhodamine B-doped silica nanoparticles. *Opt Mater* 31(11):1715–1719. doi:10.1016/j.optmat.2009.05.004
- Grasset F, Dorson F, Cordier S, Molard Y, Perrin C, Marie AM, Sasaki T, Haneda H, Bando Y, Mortier M (2008) Water-in-oil microemulsion preparation and characterization of Cs-2 Mo6X14 @SiO₂ phosphor nanoparticles based on transition metal clusters (X = Cl, Br, and I). *Adv Mater* 20(1):143. doi:10.1002/adma.200701686
- Guli M, Chen Y, Li XT, Zhu GS, Qiu SL (2007) Fluorescence of postgrafting rhodamine B in the mesopores of rodlike SBA-15. *J Lumin* 126(2):723–727. doi:10.1016/j.jlumin.2006.11.003
- He Q, Shi J, Cui X, Zhao J, Chen Y, Zhou J (2009) Rhodamine B-co-condensed spherical SBA-15 nanoparticles: facile co-condensation synthesis and excellent fluorescence features. *J Mater Chem* 19(21):3395–3403. doi:10.1039/b900357f
- Huh S, Wiench JW, Yoo JC, Pruski M, Lin VSY (2003) Organic functionalization and morphology control of mesoporous silicas via a co-condensation synthesis method. *Chem Mater* 15(22):4247–4256. doi:10.1021/cm0210041
- Lee SJ, Choi M-C, Park SS, Ha C-S (2011) Synthesis and characterization of hybrid films of polyimide and silica hollow spheres. *Macromol Res* 19(6):599–607. doi:10.1007/s13233-011-0603-8
- Li XD, Zhai QZ, Zou MQ (2010) Optical properties of (nanometer MCM-41)-(malachite green) composite materials. *Appl Surf Sci* 257(3):1134–1140. doi:10.1016/j.apsusc.2010.08.053
- Ma DL, Kell AJ, Tan S, Jakubek ZJ, Simard B (2009) Photo-physical properties of dye-doped silica nanoparticles bearing different types of dye-silica interactions. *J Phys Chem C* 113(36):15974–15981. doi:10.1021/jp905812f
- Michalet X, Pinaud FF, Bentolila LA, Tsay JM, Doose S, Li JJ, Sundaresan G, Wu AM, Gambhir SS, Weiss S (2005) Quantum dots for live cells, in vivo imaging, and diagnostics. *Science* 307(5709):538–544. doi:10.1126/science.1104274
- Nakamura K, Yamanaka K, Shikata T (2003) Hybrid threadlike micelle formation between a surfactant and polymer in aqueous solution. *Langmuir* 19(21):8654–8660. doi:10.1021/la030101l
- Nan AJ, Bai X, Son SJ, Lee SB, Ghandehari H (2008) Cellular uptake and cytotoxicity of silica nanotubes. *Nano Lett* 8(8):2150–2154. doi:10.1021/nl0802741
- Nandiyanto ABD, Kim SG, Iskandar F, Okuyama K (2009) Synthesis of spherical mesoporous silica nanoparticles with nanometer-size controllable pores and outer diameters. *Microporous Mesoporous Mater* 120(3):447–453. doi:10.1016/j.micromeso.2008.12.019
- Quemeneur F, Rinaudo M, Pepin-Donat B (2008) Influence of molecular weight and pH on adsorption of chitosan at the surface of large and giant vesicles. *Biomacromolecules* 9(1):396–402. doi:10.1021/bm700943j
- Rocha LA, Caiut JMA, Messaddeq Y, Ribeiro SJL, Martines MAU, Freiria JD, Dexpert-Ghys J, Verelst M (2010)

- Non-leachable highly luminescent ordered mesoporous SiO₂ spherical particles. *Nanotechnology* 21(15):155603. doi:[10.1088/0957-4484/21/15/155603](https://doi.org/10.1088/0957-4484/21/15/155603)
- Shibata S, Taniguchi T, Yano T, Yamane M (1997) Formation of water-soluble dye-doped silica particles. *J Sol-Gel Sci Technol* 10(3):263–268. doi:[10.1023/a:1018369200282](https://doi.org/10.1023/a:1018369200282)
- Stein A, Melde BJ, Schroden RC (2000) Hybrid inorganic-organic mesoporous silicates–nanoscopic reactors coming of age. *Adv Mater* 12(19):1403–1419. doi:[10.1002/1521-4095\(200010\)12:19<1403:aid-adma1403>3.3.co;2-o](https://doi.org/10.1002/1521-4095(200010)12:19<1403:aid-adma1403>3.3.co;2-o)
- Thomassen LCJ, Aerts A, Rabolli V, Lison D, Gonzalez L, Kirsch-Volders M, Napierska D, Hoet PH, Kirschhock CEA, Martens JA (2010) Synthesis and characterization of stable monodisperse silica nanoparticle sols for in vitro cytotoxicity testing. *Langmuir* 26(1):328–335. doi:[10.1021/la902050k](https://doi.org/10.1021/la902050k)
- Tsyalkovsky V, Klep V, Ramaratnam K, Lupitskyy R, Minko S, Luzinov I (2008) Fluorescent reactive core–shell composite nanoparticles with a high surface concentration of epoxy functionalities. *Chem Mater* 20(1):317–325. doi:[10.1021/cm0718421](https://doi.org/10.1021/cm0718421)
- Vanblaaderen A, Vrij A (1992) Synthesis and characterization of colloidal dispersions of fluorescent monodisperse silica spheres. *Langmuir* 8(12):2921–2931. doi:[10.1021/la00048a013](https://doi.org/10.1021/la00048a013)
- Wang YJ, Price AD, Caruso F (2009) Nanoporous colloids: building blocks for a new generation of structured materials. *J Mater Chem* 19(36):6451–6464. doi:[10.1039/b901742a](https://doi.org/10.1039/b901742a)
- Wang Y, Li ZH, Zhong WY, Li H, Xu DK, Chen HY (2010) Rhodamine B doped silica nanoparticle labels for protein microarray detection. *Sci China Chem* 53(4):747–751. doi:[10.1007/s11426-010-0104-1](https://doi.org/10.1007/s11426-010-0104-1)
- Xie CJ, Yin DG, Li J, Zhang L, Liu BH, Wu MH (2010) Preparation of a novel type of fluorescein isothiocyanate doped fluorescent silica nanoparticles and its application as pH probe. *Chin J Anal Chem* 38(4):488–492. doi:[10.3724/sp.j.1096.2010.00488](https://doi.org/10.3724/sp.j.1096.2010.00488)
- Yao G, Wang L, Wu YR, Smith J, Xu JS, Zhao WJ, Lee EJ, Tan WH (2006) FloDots: luminescent nanoparticles. *Anal Bioanal Chem* 385(3):518–524. doi:[10.1007/s00216-006-0452-z](https://doi.org/10.1007/s00216-006-0452-z)
- Zhao XJ, Bagwe RP, Tan WH (2004) Development of organic-dye-doped silica nanoparticles in a reverse microemulsion. *Adv Mater* 16(2):173. doi:[10.1002/adma.200305622](https://doi.org/10.1002/adma.200305622)